Int. J. Heat Mass Transfer. Vol. 33, No. 12, pp. 2651–2658, 1990
Printed in Great Britain

0017-9310/90 $3.00+0.00

Radiation in cylindrical symmetry with anisotropic scattering and variable properties

J. R. TSAI and M. N. ÖZIŞIK
Mechanical and Aerospace Engineering Department, North Carolina State University, Raleigh, NC 27695-7910, U.S.A.

(*Received* 2 *May* 1989 *and in final form* 29 *January* 1990)

Abstract—Effects of spatially varying absorption and scattering coefficients in radiation transfer in absorbing, emitting anisotropically scattering hollow and solid cylinders having reflecting boundaries are investigated. S_4 and S_6 discrete-ordinate methods have been used to solve the problem. Tabulated results are presented for the incident radiation, net radiation heat flux, the hemispherical reflectivity and transmissivity, and the exit intensity.

1. INTRODUCTION

THERE are numerous engineering applications of radiative transfer in absorbing, emitting and anisotropically scattering media with variable radiation properties. Examples include, among others, coal-fired combustion systems, light weight fibrous insulations, and heat transfer systems containing small scattering particles. Some works are available on radiation transfer in participating axisymmetrical enclosures; but they all consider constant radiation properties [1–5]. Some works are also available for the case of spatially varying albedos; but they are for a plane-parallel or spherically symmetric medium [6–12]. No work appears to be available on the solution of radiation transfer in cylindrical symmetry allowing for the spatial variation of radiation properties.

In the present study, the discrete-ordinate method [3–5, 13–17] is used to solve one-dimensional radiation transfer in cylindrically symmetric non-homogeneous hollow and solid cylinders; the accuracy and efficiency of S_4 and S_6 schemes are examined, and forward and backward scattering cases are considered.

2. FORMULATION OF THE PROBLEM

The mathematical formulation of the problem includes a sufficiently general conservative form of the equation of radiative transfer for a solid or hollow cylinder given by [18]

$$\frac{\mu}{r}\frac{\partial}{\partial r}[rI(r,\mathbf{\Omega})]-\frac{1}{r}\frac{\partial}{\partial\phi}[\eta I(r,\mathbf{\Omega})]+\beta(r)I(r,\mathbf{\Omega})$$

$$=\kappa(r)I_b(T)+\frac{\sigma(r)}{4\pi}\int_{\Omega'=4\pi}p(\mathbf{\Omega}',\mathbf{\Omega})I(r,\mathbf{\Omega}')\,d\Omega',$$

$$\text{in}\quad a_1<r<a_2 \quad (1a)$$

subjected to externally incident radiation, emission and diffuse reflection at both boundaries

$$I(a_1,\mathbf{\Omega})=(1-c)\left[f_1(\mu)+\varepsilon_1 I_{b,1}-\frac{\rho_1}{\pi}\int_{\mu'<0}I(a_1,\mathbf{\Omega}')\mu'\,d\Omega'\right]+cI(a_1,\mathbf{\Omega}'),$$

$$\text{at}\quad r=a_1,\quad \mu>0 \quad (1b)$$

$$I(a_2,\mathbf{\Omega})=f_2(\mu)+\varepsilon_2 I_{b,2}+\frac{\rho_2}{\pi}\int_{\mu'>0}I(a_2,\mathbf{\Omega}')\mu'\,d\Omega'],$$

$$\text{at}\quad r=a_2,\quad \mu<0 \quad (1c)$$

where the coefficients c, a_1 and a_2 are defined as follows:

hollow cylinder: $c=0$, $a_1=$ inner radius, $a_2=$ outer radius;
solid cylinder: $c=1$, $a_1=0$, $a_2=$ radius.

Here $I(r,\mathbf{\Omega})$ is the radiation intensity; r the space variable in the radial direction; μ, η and ξ the direction cosines of the unit vector $\mathbf{\Omega}$, i.e.

$$\mu=\sin\theta\cos\phi$$

$$\eta=\sin\theta\sin\phi$$

$$\xi=\cos\theta \quad (1d)$$

where θ and ϕ are the polar and azimuthal angles, respectively. Clearly the mathematical formulation given above will include the problems of hollow and solid cylinders if the coefficients c, a_1 and a_2 are selected as stated above. In addition, $\kappa(r)$, $\sigma(r)$ and $\beta(r)$ are the space-dependent absorption, scattering and extinction coefficients, respectively, which are related by

$$\beta(r)=\kappa(r)+\sigma(r). \quad (2)$$

The blackbody radiation intensity $I_b(T)$ is related to the temperature $T(r)$ in the medium by

$$I_b(T)=n^2\bar{\sigma}T^4(r)/\pi \quad (3)$$

NOMENCLATURE

a	positions at boundaries
A	area defined by equation (10c)
b	thickness, $a_2 - a_1$
c	coefficient in equation (1b)
d_l	expansion coefficients defined by equation (4)
$f(\mu)$	externally incident radiation at boundaries
$G(r)$	incident radiation
$I(r, \mathbf{\Omega})$	radiation intensity
L	order of anisotropic scattering in equation (4)
M	total number of discrete ordinates
$p(\mathbf{\Omega}, \mathbf{\Omega}')$	anisotropic scattering phase function defined by equation (4)
$P_l(v)$	Legendre polynomials
$q(r)$	net radiation heat flux
r	space variable in the radial direction
S^*	source function defined by equation (10b)
$T(r)$	temperature in the medium
V	control volume defined by equation (10c)
w	weight in equation (5a)
x	r/b.

Greek symbols

α	constants defined by equation (9)
$\beta(r)$	extinction coefficient
γ	coefficient defined by equation (12b)
ε	emissivities at the boundaries
$\kappa(r)$	absorption coefficient
μ, η, ξ	direction cosines defined by equation (1d)
v	$\mu\mu' + \eta\eta' + \xi\xi'$
ρ	reflectivities at the boundaries
$\sigma(r)$	scattering coefficient
$\bar{\sigma}$	Stefan–Boltzmann constant
Ω	solid angle
$\mathbf{\Omega}$	unit vector in the direction of propagation.

Subscripts

1	position at the inner radius for the hollow cylinder or at the center of the solid cylinder
2	position at the outer radius for the hollow cylinder or at the radius for the solid cylinder
b	blackbody
i	mesh points in the space coordinate
m	directions used in discrete-ordinate equations.

Superscripts

0	position at the cell center
+	positive μ-directions
−	negative μ-directions.

where n is the refractive index and $\bar{\sigma}$ the Stefan–Boltzmann constant. The anisotropic scattering phase function $p(\mathbf{\Omega}, \mathbf{\Omega}')$ is defined by

$$p(\mathbf{\Omega}, \mathbf{\Omega}') = \sum_{l=0}^{L} d_l P_l(v), \quad d_0 = 1 \tag{4}$$

where $v = \mathbf{\Omega} \cdot \mathbf{\Omega}' = \mu\mu' + \eta\eta' + \xi\xi'$, d_l are the expansion coefficients, $P_l(v)$ the Legendre polynomials and L the order of anisotropic scattering. Clearly, $L = 0$ corresponds to isotropic scattering. In the boundary conditions given by equations (1b) and (1c), $f(\mu)$ is the externally incident radiation, ε and ρ the diffuse emissivity and reflectivity of the surface, respectively, and subscripts 1 and 2 refer to the boundaries at $r = a_1$ and a_2, respectively. The geometries and coordinates for the hollow cylinder and solid cylinder are shown in Fig. 1.

The discrete-ordinate representation of equation (1a) for a finite number of discrete ordinates can be written by [5]

$$\frac{\mu_m}{r} \frac{\partial}{\partial r}[r I_m] - \frac{1}{r} \frac{\partial}{\partial \phi}[\eta_m I_m] + \beta(r) I_m = \kappa(r) I_b + \frac{\sigma(r)}{4\pi} \sum_{m'} w_{m'} p_{mm'} I_{m'} \tag{5a}$$

where $I_m = I(r, \mathbf{\Omega})$, subscripts m and m' represent the discrete directions, w_m the weight, and $p_{mm'}$ is given by

$$p_{mm'} = \sum_{l=0}^{L} a_l P_l(v_{mm'}) \tag{5b}$$

and

$$v_{mm'} = \mu_m \mu_{m'} + \eta_m \eta_{m'} + \xi_m \xi_{m'}. \tag{5c}$$

The discrete-ordinate representation of the boundary conditions, equations (1b) and (1c), is given by

$$I_m = (1-c)\left[f_{1,m} + \varepsilon_1 I_{b,1} - \frac{\rho_1}{\pi} \sum_{m'} w_{m'} \mu_{m'} I_{m'} \right] + c I_{m'};$$
$$\mu_m > 0, \quad \mu_{m'} < 0, \quad r = a_1 \tag{6a}$$

$$I_m = f_{2,m} + \varepsilon_2 I_{b,2} + \frac{\rho_2}{\pi} \sum_{m'} w_{m'} \mu_{m'} I_{m'};$$
$$\mu_m < 0, \quad \mu_{m'} > 0, \quad r = a_2. \tag{6b}$$

If equation (5a) is integrated over all angles, the second term on the left-hand side vanishes. By direct differencing, we define the discrete form of the term $\partial(\eta I_m)/\partial\phi$ for a particular value of ξ_m as [3]

$$\frac{\partial}{\partial \phi}(\eta I_m) = \frac{\alpha_{m+1/2} I_{m+1/2} - \alpha_{m-1/2} I_{m-1/2}}{w_m} \tag{7}$$

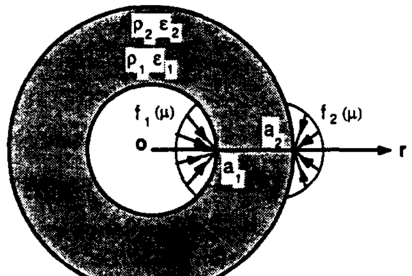

(a)

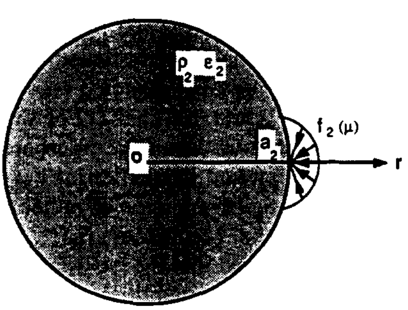

(b)

FIG. 1. Top views of the geometries and coordinates for the hollow (a) and solid cylinders (b).

where $I_{m+1/2}$ and $I_{m-1/2}$ are the intensities in the directions of $m+1/2$ and $m-1/2$, respectively, and the constants $\alpha_{m+1/2}$ and $\alpha_{m-1/2}$ are yet to be determined. Equation (7) is now introduced into equation (5a)

$$\frac{\mu_m}{r}\frac{\partial}{\partial r}(rI_m)-\frac{\alpha_{m+1/2}I_{m+1/2}-\alpha_{m-1/2}I_{m-1/2}}{rw_m}+\beta(r)I_m = \kappa(r)I_b+\frac{\sigma(r)}{4\pi}\sum_{m'} w_{m'}p_{mm'}I_{m'}. \quad (8)$$

This equation has no angular derivative but includes unknown constants $\alpha_{m+1/2}$ and $\alpha_{m-1/2}$. These constants can be determined by considering the case of the conservative medium, i.e. $\sigma/\beta = 1$. For such a case, $I_{m+1/2} = I_{m-1/2} = I_m =$ constant, and equation (8) reduces to

$$\alpha_{m+1/2}-\alpha_{m-1/2} = \mu_m w_m. \quad (9)$$

This expression provides a recursion relation for determining the constants $\alpha_{m+1/2}$ and $\alpha_{m-1/2}$ for each particular value of ξ_m.

3. METHOD OF SOLUTION

The discrete-ordinate equation (7) can be solved as now described. Equation (8) is multiplied by $2\pi r\,dr$ and integrated over the cell from $r = r_i$ to r_{i+1} to obtain

$$\mu_m(A_{i+1}I_{m,i+1}-A_iI_{m,i})-(A_{i+1}-A_i)\times\left[\frac{\alpha_{m+1/2}I^0_{m+1/2}-\alpha_{m-1/2}I^0_{m-1/2}}{w_m}\right]+\beta^0V^0I^0_m = V^0S^*_m \quad (10a)$$

where

$$S^*_m = \kappa^0I^0_b+\frac{\sigma^0}{4\pi}\sum_{m'} w_{m'}p_{mm'}I^0_{m'} \quad (10b)$$

$$A_i = 2\pi r_i,\quad V^0 = \pi(r^2_{i+1}-r^2_i) \quad (10c)$$

and the quantities with a superscript 0 denote the values at the node centre, i.e. $i+1/2$.

The intensity at the cell centre I^0_m is related to the intensities $I_{m,i}$ and $I_{m,i+1}$ at the cell boundaries i and $i+1$ by

$$I^0_m = \tfrac{1}{2}(I_{m,i}+I_{m,i+1}) \quad (11a)$$

and the intensity I^0_m is also related to the intensities $I^0_{m-1/2}$ and $I^0_{m+1/2}$ at the angular edges $m-1/2$ and $m+1/2$ by

$$I^0_m = \tfrac{1}{2}(I^0_{m-1/2}+I^0_{m+1/2}). \quad (11b)$$

The computation of equations (10a) and (10b) is performed from $r = a_2$ to a_1 (i.e. inwards) for $\mu_m < 0$ and from $r = a_1$ to a_2 (i.e. outwards) for $\mu_m > 0$ as described below.

(1) $\mu_m < 0$ (inward calculations): eliminating $I_{m,i}$ and $I^0_{m+1/2}$ from equations (10a) and (10b) by utilizing the expressions given by equations (11a) and (11b) we obtain

$$I^0_m = \frac{-\mu_mAI_{m,i+1}+\gamma^0_mI^0_{m-1/2}+V^0S^*_m}{-\mu_mA+\gamma^0_m+\beta^0V^0},\quad \mu_m<0 \quad (12a)$$

where

$$A = A_i+A_{i+1} \quad (12b)$$

$$\gamma^0_m = -(\alpha_{m-1/2}+\alpha_{m+1/2})(A_{i+1}-A_i)/w_m. \quad (12c)$$

(2) $\mu_m > 0$ (outward calculations): eliminating $I_{m,i+1}$ and $I^0_{m+1/2}$ from equations (10a) and (10b) by using the expressions given by equations (11a) and (11b), we find

$$I^0_m = \frac{\mu_mAI_{m,i}+\gamma^0_mI^0_{m-1/2}+V^0S^*_m}{\mu_mA+\gamma^0_m+\beta^0V^0},\quad \mu_m>0 \quad (13)$$

where the quantities A and γ^0_m have been defined in equations (12b) and (12c).

Note that the calculations of equations (12) and (13) require an initial estimate of the intensity $I^0_{m-1/2}$ for each particular value of ξ_m. This can be found by solving equations (12) in the direction of $\eta_m = 0$ and setting $\mu_m = (1-\xi^2_m)^{1/2}$, where the azimuthally angular derivative vanishes [19]. The solution of equations (12) and (13) must be obtained iteratively due to the unknown terms for the reflection in the boundaries and in-scattering in the medium. Therefore, reflection terms in equations (6a) and (6b) and in-scattering term in equation (10b) are set equal to zero, thus both terms are regarded known in the first calculation and updated in the following iterations. The procedure is continued until the convergence criterion $|I^{(i+1)} - I^{(i)}| < 10^{-6}$ is achieved, where superscript (i) refers to the iteration level.

The accuracy of the discrete-ordinate solutions depends on the choice of the quadrature scheme. Recently, Fiveland [14] showed that Gaussian quadratures used in the calculation results in the inaccurate solutions because these quadrature points do not satisfy the first moment for half range. In this work, the moment-matching technique proposed by Carlson and Lathrop [19], is applied to calculate the quadrature points and weights. The quadrature scheme should satisfy the zeroth and second moments for full range (i.e. 4π); and the first moment for half range (i.e. 2π). The total number of the discrete ordinates M is identical to $N(N+2)/4$ when S_N schemes are used for one-dimensional cylindrical geometry. The quadrature points and weights for S_4 and S_6 schemes are listed in Table 1.

Finally, the incident radiation G_i, the net radiation heat flux q_i and the forward and backward radiation fluxes q_i^+ and q_i^- anywhere in the medium are determined from

$$G_i = \sum_{m=1}^{M} w_m I_{m,i} \quad (14)$$

$$q_i = \sum_{m=1}^{M} \mu_m w_m I_{m,i} \quad (15)$$

$$q_i^+ = \sum_{\mu_m > 0} \mu_m w_m I_{m,i} \quad (16a)$$

$$q_i^- = \sum_{\mu_m < 0} \mu_m w_m I_{m,i}. \quad (16b)$$

Table 1. Quadrature points and weights for S_4 and S_6 schemes

m	μ_m	η_m	ξ_m	w_m
		S_4		
1	−0.295876	0.295876	−0.908248	$2\pi/3$
2	0.295876	0.295876	−0.908248	$2\pi/3$
3	−0.908248	0.295876	−0.295876	$2\pi/3$
4	−0.295876	0.908248	−0.295876	$2\pi/3$
5	0.295876	0.908248	−0.295876	$2\pi/3$
6	0.908248	0.295876	−0.295876	$2\pi/3$
		S_6		
1	−0.224556	0.224556	−0.948235	$\pi/3$
2	0.224556	0.224556	−0.948235	$\pi/3$
3	−0.689048	0.224556	−0.689048	$\pi/3$
4	−0.224556	0.689048	−0.689048	$\pi/3$
5	0.224556	0.689048	−0.689048	$\pi/3$
6	0.689048	0.224556	−0.689048	$\pi/3$
7	−0.948235	0.224556	−0.224556	$\pi/3$
8	−0.689048	0.689048	−0.224556	$\pi/3$
9	−0.224556	0.948235	−0.224556	$\pi/3$
10	0.224556	0.948235	−0.224556	$\pi/3$
11	0.689048	0.689048	−0.224556	$\pi/3$
12	0.948235	0.224556	−0.224556	$\pi/3$

4. RESULTS AND DISCUSSION

In this work, we solved the radiation problem with spatially varying radiation properties for the hollow and solid cylinders. For the purpose of comparison with available data in the literature, the extinction coefficient is chosen as unity, i.e. $\beta(r) = 1$, and the scattering coefficient $\sigma(r)$ is varied for all the cases. To show the effects of the anisotropic scattering, two different scattering laws [20], one representing forward scattering and the other backward scattering, are considered and the corresponding coefficients d_l of equation (4) are listed in Table 2. For simplicity, we assume that the boundaries are transparent (i.e. $\rho_1 = \rho_2 = 0$), no external irradiation at $r = a_1$ (i.e. $f_1(\mu) = 0$), and negligible emission of radiation from the medium and the boundaries (i.e. $I_b = I_{b,1} = I_{b,2} = 0$). It is to be noted that the inclusion in the analysis of any one of the quantities just mentioned does not pose any computational difficulty. The units for a_1 and a_2 and b should be in consistent units, i.e. in meters (m), if the radiation properties $\kappa(r)$, $\sigma(r)$ and $\beta(r)$ are in m^{-1}. Both S_4 and S_6 schemes are used to obtain the results given in Tables 3 and 4 while only the S_6 scheme is chosen to obtain the results in Tables 6–9.

Tables 3 and 4 show the incident radiation and the net radiation heat flux, respectively, for an isotropically scattering, solid cylinder obtained by the S_4 and S_6 schemes compared with those obtained by the F_N method [21] that can be considered 'exact'. The results of the S_6 scheme are in good agreement with the exact solutions and more accurate than those of the S_4 scheme in general. However, the S_4 scheme is

Table 2. A forward (refractive index = 1.2, size parameter† = 2) and a backward (refractive index = ∞, size parameter = 1) scattering law used in the calculations

l	Forward scattering	Backward scattering
0	1.0	1.0
1	1.98398	−0.56524
2	1.50823	0.29783
3	0.70075	0.08571
4	0.23489	0.01003
5	0.05133	0.00063
6	0.00760	0.00000
7	0.00048	
8	0.00000	

†Size parameter is defined by $\pi D/\lambda$, where D is the diameter of the scattering particle and λ the wavelength of the incident radiation.

Table 3. Incident radiations G of the solid cylinder at $x = r/b = 0.5$ and 1 with a transparent boundary and $f_2(\mu) = 1$

$\sigma(r)$	b	S_4	S_6	Exact[21]
		(a) $G(x = 0.5)/4\pi$, $x = r/b$		
	1	0.620040	0.630505	0.636839
0.7	5	0.091478	0.092803	†
	10	0.010558	0.010720	0.010452
	1	0.710137	0.721582	0.727408
0.8	5	0.147595	0.150245	†
	10	0.022849	0.023542	0.023259
	1	0.826551	0.839541	0.844174
0.9	5	0.288350	0.294015	†
	10	0.070782	0.073396	0.073336
		(b) $G(x = 1)/4\pi$, $x = r/b$		
	1	0.815985	0.816584	0.819473
0.7	5	0.679323	0.680391	†
	10	0.661876	0.662740	0.663331
	1	0.864551	0.864265	0.866527
0.8	5	0.728325	0.729167	†
	10	0.708407	0.709251	0.709789
	1	0.925081	0.923651	0.924929
0.9	5	0.804852	0.805184	†
	10	0.780121	0.780808	0.781243

†No exact data are available in the literature.

Table 4. Net radiation heat fluxes of the solid cylinder at $x = r/b = 0.5$ and 1 with a transparent boundary and $f_2(\mu) = 1$

$\sigma(r)$	b	S_4	S_6	Exact[21]
		(a) $-q(x = 0.5)$, $x = r/b$		
	1	0.538040	0.573512	0.580910
0.7	5	0.278374	0.296689	†
	10	0.040422	0.042486	0.041055
	1	0.411955	0.441731	0.446820
0.8	5	0.322294	0.348391	†
	10	0.065848	0.070595	0.069274
	1	0.240567	0.259596	0.262105
0.9	5	0.351241	0.384240	†
	10	0.126141	0.137024	0.136417
		(b) $-q(x = 1)$, $x = r/b$		
	1	1.271199	1.289640	1.298940
0.7	5	2.166435	2.182758	†
	10	2.247395	2.262108	2.276860
	1	0.944730	0.959169	0.964758
0.8	5	1.859101	1.875275	†
	10	1.963641	1.978000	1.990130
	1	0.534440	0.543147	0.545307
0.9	5	1.359231	1.374945	†
	10	1.509325	1.522666	1.530480

†No exact data are available in the literature.

more efficient than the S_6 scheme. The number of control volumes V^0 in the r-direction (# C.V.) and the CPU time (in seconds (s)) consumed by an IBM 3081 system for the S_4 and S_6 schemes for the calculations of Tables 3 and 4 are listed in Table 5. Experience shows the number of control volumes should be increased with increasing the radius of the cylinder for the sake of accuracy. As expected, the CPU time increases with increasing the values of the radius b. For the non-scattering case, i.e. $\sigma(r) = 0$, the CPU time consumed by the S_4 and S_6 schemes are not much different. However, the S_6 scheme consumes

Table 5. Number of control volumes and CPU times for the S_4 and S_6 schemes

b	$\sigma(r)$	$S_4(M = 6)$ # C.V.	$S_4(M = 6)$ CPU (s)	$S_6(M = 12)$ # C.V.	$S_6(M = 12)$ CPU (s)
1	0.0	7	1.8	15	1.9
	0.7	7	2.0	15	3.4
5	0.0	35	1.9	75	2.5
	0.7	35	3.9	75	15.5
10	0.0	70	2.0	150	3.3
	0.7	70	5.7	150	28.3

Table 6. Effects of spatial variation of scattering coefficient, $\sigma(r)$, on hemispherical reflectivity and transmissivity of a hollow cylinder with $a_1 = 1$, $b = 1$, transport boundaries and $f_2(\mu) = 1$. $\{F_1 = (a_2^3-a_1^3)/(a_2^2-a_1^2)$ and $F_2 = (a_2^4-a_1^4)/(a_2^2-a_1^2)\}$

$\sigma(r)$	Forward scattering Reflectivity	Forward scattering Transmissivity	Isotropic scattering Reflectivity	Isotropic scattering Transmissivity	Backward scattering Reflectivity	Backward scattering Transmissivity
			Linear variation of $\sigma(r)$			
$3r/4F_1$	0.100764	0.312083	0.128576	0.291873	0.136387	0.286632
$0.2+9r/20F_1$	0.125505	0.361238	0.165666	0.320213	0.176618	0.309965
$0.4+3r/20F_1$	0.157142	0.420879	0.209481	0.355777	0.223219	0.339966
0.5	0.176410	0.455613	0.234630	0.377147	0.249598	0.358313
$0.6-3r/20F_1$	0.198620	0.494317	0.262474	0.401566	0.278544	0.379533
$0.8-9r/20F_1$	0.254631	0.586500	0.328558	0.462450	0.346391	0.433469
$1-3r/4F_1$	0.333034	0.705251	0.414412	0.546873	0.433349	0.510330
			Quadratic variation of $\sigma(r)$			
$3r/8F_1+r^2/2F_2$	0.088410	0.297486	0.109272	0.283555	0.115212	0.279892
$0.4-9r/40F_1+r^2/2F_2$	0.138560	0.399541	0.184028	0.342846	0.196183	0.328994
$0.6-21r/40F_1+r^2/2F_2$	0.175060	0.467952	0.232375	0.384819	0.247060	0.364990
$1-9r/8F_1+r^2/2F_2$	0.291482	0.662127	0.368150	0.515399	0.386192	0.481535

Table 7. Effects of spatial variation of scattering coefficient, $\sigma(x)$, on hemispherical reflectivity of a solid cylinder with $a_2 = 1$, transparent boundary and $f_2(\mu) = 1$

$\sigma(x)$, $x = r/b$	Forward scattering	Isotropic scattering	Backward scattering
	Linear variation of $\sigma(x)$		
$3x/4$	0.445810	0.468708	0.475870
$0.2+9x/20$	0.432647	0.452524	0.458903
$0.4+3x/20$	0.421450	0.438191	0.443747
0.5	0.416603	0.431747	0.436880
$0.6-3x/20$	0.412265	0.425805	0.430509
$0.8-9x/20$	0.405181	0.415520	0.419352
$1-3x/4$	0.400336	0.407567	0.410530
	Quadratic variation of $\sigma(x)$		
$3x/8+x^2/2$	0.458570	0.484055	0.491929
$0.4-9x/40+x^2/2$	0.431130	0.450650	0.456960
$0.6-21x/40+x^2/2$	0.420409	0.436768	0.442239
$1-9x/8+x^2/2$	0.405276	0.415245	0.418971

much more computation time that the S_4 scheme for $\sigma(r) = 0.7$.

Table 6 lists the hemispherical reflectivity $q^+(a_2)/\pi$ and transmissivity $q^-(a_1)/\pi$ for the hollow cylinder while Table 7 shows the hemispherical reflectivity $q^+(a_2)/\pi$ for the solid cylinder subjected to an isotropic incidence of unit strength at $r = a_2$. The values of the thickness $b(=a_2-a_1)$ are considered 1 in both tables in the case of $a_1 = 1$ and 0 for Tables 6 and 7, respectively. To illustrate the effects of the spatial variation of the scattering coefficient on the hemispherical reflectivity and transmissivity, we have chosen seven linear and four quadratic variations of $\sigma(r)$ having the average value of 0.5 over the region $a_1 \leqslant r \leqslant a_2$ in the hollow and solid cylinders. The effects of forward, isotropic and backward scattering are also shown in Tables 6 and 7.

Table 8. Exit distribution of radiation intensity I_m^- at $r = a_1$ and I_m^+ at $r = a_2$ of a hollow cylinder with transparent boundaries and $f_2(\mu) = 1$

b	$I_m^\pm$	m	$\sigma(r)$, $F_1 = (a_2^3-a_1^3)/(a_2^2-a_1^2)$: $3r/4F_1$	0.5	$1-3r/4F_1$
			(a) Forward scattering		
1	$I_m^-(a_1)$	1	0.0380	0.1668	0.4669
		3	0.2866	0.4314	0.6867
		4	0.1890	0.3259	0.5988
		7	0.4048	0.5503	0.7796
		8	0.3572	0.5035	0.7490
		9	0.2577	0.4039	0.6721
	$I_m^+(a_2)$	2	0.1352	0.2430	0.4367
		5	0.3399	0.4341	0.5812
		6	0.0211	0.0837	0.2578
		10	0.5301	0.6067	0.7156
		11	0.0879	0.1998	0.4114
		12	0.0172	0.0607	0.1843
3	$I_m^-(a_1)$	1	0.0004	0.0333	0.3699
		3	0.0196	0.0892	0.5014
		4	0.0120	0.0669	0.4425
		7	0.0546	0.1501	0.5785
		8	0.0457	0.1325	0.5548
		9	0.0313	0.1030	0.5010
	$I_m^+(a_2)$	2	0.0688	0.1978	0.5180
		5	0.1736	0.3033	0.5868
		6	0.0112	0.0648	0.3736
		10	0.3165	0.4419	0.6866
		11	0.0106	0.0743	0.4114
		12	0.0060	0.0462	0.3357
			Table 8—*Continued.*		
			(b) Isotropic scattering		
1	$I_m^-(a_1)$	1	0.0362	0.1439	0.3728
		3	0.2685	0.3593	0.5389
		4	0.1766	0.2691	0.4605
		7	0.3791	0.4574	0.6100
		8	0.3335	0.4146	0.5766
		9	0.2398	0.3278	0.5086
	$I_m^+(a_2)$	2	0.1607	0.2885	0.4881
		5	0.3507	0.4521	0.6012
		6	0.0551	0.1593	0.3612
		10	0.5292	0.6052	0.7131
		11	0.1098	0.2363	0.4484
		12	0.0535	0.1432	0.3091
3	$I_m^-(a_1)$	1	0.0004	0.0208	0.2108
		3	0.0172	0.0494	0.2819
		4	0.0105	0.0369	0.2424
		7	0.0485	0.0856	0.3227
		8	0.0407	0.0748	0.3033
		9	0.0278	0.0571	0.2694
	$I_m^+(a_2)$	2	0.0860	0.2500	0.5736
		5	0.1853	0.3384	0.6258
		6	0.0365	0.1527	0.4766
		10	0.3214	0.4568	0.7006
		11	0.0305	0.1445	0.4846
		12	0.0334	0.1442	0.4524
			(c) Backward scattering		
1	$I_m^-(a_1)$	1	0.0344	0.1306	0.3433
		3	0.2633	0.3400	0.5021
		4	0.4279	0.1729	0.2534
		7	0.3728	0.4367	0.5711
		8	0.3278	0.3954	0.5393
		9	0.2355	0.3122	0.4772
	$I_m^+(a_2)$	2	0.1642	0.2947	0.4964
		5	0.3539	0.4577	0.6086
		6	0.0633	0.1749	0.3808
		10	0.5318	0.6098	0.7192
		11	0.1175	0.2498	0.4649
		12	0.0640	0.1644	0.3355
3	$I_m^-(a_1)$	1	0.0003	0.0167	0.1812
		3	0.0165	0.0419	0.2431
		4	0.0101	0.0311	0.2085
		7	0.0474	0.0763	0.2804
		8	0.0397	0.0665	0.2630
		9	0.0272	0.0506	0.2345
	$I_m^+(a_2)$	2	0.0887	0.2582	0.5825
		5	0.1878	0.3458	0.6343
		6	0.0432	0.1717	0.4943
		10	0.3233	0.4629	0.7080
		11	0.0363	0.1618	0.5015
		12	0.0425	0.1703	0.4766

In Tables 8 and 9, we present the results for the exit intensities I^- at $r = a_1$ and I^+ at $r = a_2$ for the hollow cylinder and I^+ at $r = a_2$ for the solid cylinder, respectively, for the case of the unit isotropic incidence at $r = a_2$. The scattering coefficients having the average

Table 9. Exit distribution of radiation intensity I_m^+ at $r = a_2$ of a solid cylinder with a transparent boundary and $f_2(\mu) = 1$

b	m	$\sigma(x)$, $x = r/b$		
		$3x/4$	0.5	$1-3x/4$
		(a) Forward scattering		
1	2	0.4383	0.3524	0.2807
	5	0.7001	0.6126	0.5350
	6	0.3082	0.2949	0.2977
	10	0.8352	0.7658	0.7036
	11	0.5340	0.4619	0.3996
	12	0.3310	0.3581	0.4000
10	2	0.3083	0.1694	0.0790
	5	0.3487	0.2106	0.1199
	6	0.1192	0.0535	0.0206
	10	0.4222	0.2835	0.1885
	11	0.1173	0.0515	0.0204
	12	0.0707	0.0276	0.0093
		(b) Isotropic scattering		
1	2	0.4764	0.3847	0.3044
	5	0.7046	0.6184	0.5400
	6	0.3515	0.3272	0.3182
	10	0.8241	0.7599	0.7014
	11	0.5354	0.4639	0.4012
	12	0.3636	0.3735	0.4007
10	2	0.3921	0.2254	0.1075
	5	0.4232	0.2600	0.1448
	6	0.2657	0.1462	0.0677
	10	0.4762	0.3196	0.2068
	11	0.2557	0.1370	0.0634
	12	0.2339	0.1283	0.0595
		(c) Backward scattering		
1	2	0.4782	0.3850	0.3037
	5	0.7079	0.6202	0.5407
	6	0.3587	0.3319	0.3202
	10	0.8274	0.7619	0.7023
	11	0.5429	0.4693	0.4043
	12	0.3736	0.3815	0.4060
10	2	0.4070	0.2350	0.1123
	5	0.4374	0.2691	0.1493
	6	0.2944	0.1673	0.0798
	10	0.4891	0.3276	0.2106
	11	0.2839	0.1571	0.0748
	12	0.2705	0.1560	0.0760

value of 0.5 are considered $\sigma(r) = 3r/4F_1$, 0.5 and $1-3r/4F_1$, $F_1 = (a_2^3-a_1^3)/(a_2^2-a_1^2)$, for the hollow cylinder and $\sigma(r) = 3x/4$, 0.5 and $1-3x/4$, $x = r/b$, for the solid cylinder. The directions $m = 1, 3, 4, 7, 8$ and 9 representing $\mu_m < 0$ and $m = 2, 5, 6, 10, 11$ and 12 representing $\mu_m > 0$ for the S_6 scheme are shown in Table 1.

The ray effects mentioned in ref. [17] may affect the accuracy only in some special cases such as the line source in the medium and a collimated heat flux at the boundary.

5. CONCLUSION

The discrete-ordinate method has been used to solve the radiation problem with variable radiation properties in one-dimensional absorbing, emitting and anisotropically scattering cylindrical media. The accuracy and efficiency for the S_4 and S_6 schemes are compared. The present results show that the spatial variation of radiation properties significantly affects the hemispherical reflectivity and transmissivity and the exit intensity.

Acknowledgement—This work was supported by the Alcoa Foundation Grant of the Alcoa Technical Center, Pennsylvania.

REFERENCES

1. S. S. Dua and P. Cheng, Multi-dimensional radiative transfer in a cylindrical media with non-isothermal bounding walls, *Int. J. Heat Mass Transfer* **18**, 245–259 (1975).
2. M. P. Mengüç and R. Viskanta, Radiative transfer in axisymmetric finite cylindrical enclosures, *J. Heat Transfer* **108**, 271–276 (1986).
3. D. J. Hyde and J. S. Truelove, The discrete ordinates approximation for multidimensional radiant heat transfer in furnaces, UKAEA Report AERE-R8502, AERE Harwell, Oxfordshire, U.K. (1977).
4. A. S. Jamaluddin and P. J. Smith, Predicting radiative transfer in axisymmetric cylindrical enclosures using the discrete ordinates method, *Combust. Sci. Technol.* **62**, 173–186 (1988).
5. W. A. Fiveland, A discrete ordinates method for predicting radiative heat transfer in axisymmetric enclosures, ASME Paper No. 82-HT-20 (1982).
6. E. Simonneau, Radiative transfer in atmospheres with spherical symmetry—IV. The non-conservative problem, *J. Quant. Spectrosc. Radiat. Transfer* **23**, 73–81 (1980).
7. S. T. Thynell and M. N. Özişik, Radiation transfer in an isotropically scattering solid sphere with space dependent albedo, $\omega(r)$, *J. Heat Transfer* **107**, 732–734 (1985).
8. S. A. El-Wakil, M. H. Haggag, M. T. Attia and E. A. Saad, Radiative transfer in an inhomogeneous sphere, *J. Quant. Spectrosc. Radiat. Transfer* **40**, 71–78 (1988).
9. R. D. M. Garcia and C. E. Siewert, Radiative transfer in finite inhomogeneous plane-parallel atmospheres, *J. Quant. Spectrosc. Radiat. Transfer* **27**, 141–148 (1982).
10. Y. A. Cengel, M. N. Özişik and Y. Yener, Radiative transfer in a plane-parallel medium with space-dependent albedo, $\omega(x)$, *Int. J. Heat Mass Transfer* **27**, 1919–1921 (1984).
11. Y. A. Cengel and M. N. Özişik, Radiation transfer in an anisotropically scattering plane-parallel medium with space-dependent albedo $\omega(x)$, *J. Quant. Spectrosc. Radiat. Transfer* **34**, 263–270 (1985).
12. J. T. Tsai, M. N. Özişik and F. Santarelli, Radiation in spherical symmetry with anisotropic scattering and variable properties, *J. Quant. Spectrosc. Radiat. Transfer* **42**, 187–199 (1989).
13. W. A. Fiveland, Discrete-ordinates solutions of the radiative transport equation for rectangular enclosures, *J. Heat Transfer* **106**, 699–706 (1984).
14. W. A. Fiveland, Discrete ordinate methods for radiative heat transfer in isotropically and anisotropically scattering media, *J. Heat Transfer* **109**, 809–812 (1987).
15. J. S. Truelove, Discrete-ordinate solutions of the radiation transport equation, *J. Heat Transfer* **109**, 1048–1051 (1987).
16. J. S. Truelove, Three-dimensional radiation in absorbing–emitting–scattering media using the discrete-ordinates approximation, *J. Quant. Spectrosc. Radiat. Transfer* **39**, 27–31 (1988).
17. J. Duderstadt and W. Martin, *Transport Theory*. Wiley, New York (1979).
18. M. N. Özişik, *Radiative Transfer*. Wiley, New York (1973).
19. B. G. Carlson and K. D. Lathrop, Transport theory—

the method of discrete ordinates. In *Computing Methods in Reactor Physics* (Edited by H. Greenspan, C. N. Kelber and D. Okrent). Gordon & Breach, New York (1968).
20. C. M. Chu, G. C. Clark and S. W. Churchill, Tables of angular distribution coefficients for light scattering by spheres, University of Michigan, Ann Arbor, Michigan (1957).
21. C. E. Siewert and J. R. Thomas, Radiative transfer calculations in spheres and cylinders, *J. Quant. Spectrosc. Radiat. Transfer* **34**, 59–64 (1985).

RAYONNEMENT AVEC SYMETRIE CYLINDRIQUE, DIFFUSION ANISOTROPE ET PROPRIETES VARIABLES

Résumé—On étudie les effets sur le transfert radiatif des coefficients variables d'absorption et de diffusion pour des cylindres solides creux émettant et diffusant de façon anisotrope et ayant des frontières réfléchissantes. Des méthodes S_4 et S_6 sont utilisées pour résoudre le problème. Des résultats sont présentés sous forme de table pour le flux radiant net, la réflectivité et la transmittivité hémisphérique ainsi que l'exitance.

STRAHLUNG IN SYMMETRISCHER ZYLINDERGEOMETRIE MIT ANISOTROPER STREUUNG UND VARIABLEN EIGENSCHAFTEN

Zusammenfassung—Es werden die Einflüsse örtlich variierender Absorptions- und Streuungskoeffizienten bei der Strahlung in absorbierenden, emittierenden, anisotrop streuenden, hohlen und massiven Zylindern mit reflektierenden Oberflächen untersucht. Zur Lösung des Problems werden unterschiedliche Verfahren angewandt. Ergebnisse für die folgenden Größen werden tabellarisch dargestellt: einfallende Strahlung, Netto-Strahlungswärmefluß, Reflexions- und Transmissionvermögen (auf eine Halbkugel bezogen) und Ausgangsintensität.

ОСЕСИММЕТРИЧНОЕ ИЗЛУЧЕНИЕ ПРИ АНИЗОТРОПНОМ РАССЕЯНИИ И ПЕРЕМЕННЫХ СВОЙСТВАХ

Аннотация—Исследуется влияние переменных по пространству коэффициентов поглощения и рассеяния на радиационный перенос в поглощающих и испускающих анизотропно рассеивающих полых и сплошных цилиндрах с отражающими границами. Для решения задачи используются методы дискретных ординат S_4 и S_6. Приводятся табулированные результаты для падающего излучения, суммарного теплового потока излучения, полусферических коэффициентов отражения и пропускания, а также выходной интенсивности.